01 Jan 2003

In-Plane Anisotropy and Temperature Dependence of Oxygen Phonon Modes in $YBa_2Cu_3O_{6.95}$

Jaeho Chung

Takeshi Egami

R. J. McQueeney

Mohana Yethiraj

et. al. For a complete list of authors, see https://scholarsmine.mst.edu/matsci_eng_facwork/1739

Recommended Citation

J. Chung and T. Egami and R. J. McQueeney and M. Yethiraj and M. Arai and T. Yokoo and Y. N. Petrov and H. A. Mook and Y. Endoh and S. Tajima and C. D. Frost and F. Dogan, "In-Plane Anisotropy and Temperature Dependence of Oxygen Phonon Modes in $YBa_2Cu_3O_{6.95}$," *Physical Review B (Condensed Matter)*, vol. 67, no. 1, pp. 014517-1-014517-9, American Physical Society (APS), Jan 2003.
The definitive version is available at https://doi.org/10.1103/PhysRevB.67.014517

In-plane anisotropy and temperature dependence of oxygen phonon modes in $YBa_2Cu_3O_{6.95}$

J.-H. Chung,[1] T. Egami,[1] R. J. McQueeney,[2] M. Yethiraj,[3] M. Arai,[4] T. Yokoo,[4] Y. Petrov,[5] H. A. Mook,[3] Y. Endoh,[6] S. Tajima,[7] C. Frost,[8] and F. Dogan[9]

[1]*Department of Materials Science and Engineering and Laboratory for Research on the Structure of Matter, University of Pennsylvania, Philadelphia, Pennsylvania 19104*

[2]*Los Alamos National Laboratory, Los Alamos, New Mexico 87545*

[3]*Oak Ridge National Laboratory, Oak Ridge, Tennessee 37831*

[4]*Institute of Materials Structure Science, KEK, Tsukuba 305-0801, Japan*

[5]*Department of Physics and Astronomy, University of Pennsylvania, Philadelphia, Pennsylvania 19104*

[6]*Institute for Materials Research, Tohoku University, Sendai 980, Japan*

[7]*Superconductivity Research Laboratory, International Superconductivity Technology Center, Tokyo 135-0062, Japan*

[8]*Rutherford Appleton Laboratory, Didcot, Oxon, OX11 0QX, United Kingdom*

[9]*Department of Materials Science, University of Washington, Seattle, Washington 98195*

(Received 15 February 2002; revised manuscript received 15 August 2002; published 21 January 2003)

Inelastic pulsed neutron scattering measurements on $YBa_2Cu_3O_{6.95}$ single crystals indicate that the sample has a distinct *a*-*b* plane anisotropy in the oxygen vibrations. The Cu-O bond-stretching-type phonons, which are suspected to interact strongly with charge, are simultaneously observed along the *a* and *b* directions due to a 7-meV splitting arising from the orthorhombicity, even though the sample is twinned. The bond-stretching LO branch with the polarization along *a* (perpendicular to the chain) loses intensity beyond the middle of the zone, indicating branch splitting as seen in doped nickelates, with the second branch being located at 10 meV below. The mode along *b* has a continuous dispersion. These modes show temperature dependence, which parallels that of superconductive order parameter, suggesting significant involvement of phonons in the superconductivity of this compound.

DOI: 10.1103/PhysRevB.67.014517 PACS number(s): 74.25.Kc, 63.20.Kr, 71.30.+h, 74.20.Mn

I. INTRODUCTION

For a long time the majority opinion on the mechanism of the high-temperature superconductivity (HTSC) has been that it occurs via a purely electronic mechanism involving spin excitations, and phonons are either irrelevant or even harmful to HTSC.[1] However, in recent years evidence has been building that the lattice may play a nontrivial role in the transport and superconducting properties of HTSC cuprates.[2] In particular, the high-energy Cu-O bond-stretching modes have their frequencies strongly and abruptly reduced when crossing from the insulating to the metallic phase as a function of doping.[3–6] Photoemission also suggests strong electron-phonon interaction for these modes.[7,8] The compendium of measurements seem to support the presence of an anisotropic, locally inhomogeneous charge distribution, which may take the form of the stripes.[9,10] The present paper describes the results of inelastic neutron-scattering measurements on $YBa_2Cu_3O_{6.95}$ (YBCO) carried out at a pulsed neutron source. We show that the dispersion of Cu-O bond-stretching phonons in orthorhombic YBCO are very different along *a* and *b* directions, with the dispersion of the LO mode along *a* splitting into two, high-energy and low-energy branches. The *a* axis is also the direction of the modulation wave vector for incommensurate spin fluctuations observed in detwinned single crystals[11] establishing a connection between the Cu-O bond-stretching modes and the stripe structure. We also show that the inelastic neutron-scattering intensity from phonons changes with temperature, in a similar manner as the superconducting order parameter does. These results suggest strong involvement of phonons in the superconductivity of this compound. Parts of this work have briefly been reported elsewhere.[12–14]

II. EXPERIMENTAL RESULTS

Inelastic neutron-scattering measurements were performed on $YBa_2Cu_3O_{6.95}$ crystals by neutron time-of-flight spectroscopy on the MAPS spectrometer at the ISIS facility of Rutherford Appleton Laboratory with an incident energy of about 120 meV. The energy resolution was chosen to be about 4% of the final energy, or 5 meV for elastic scattering and 3 meV at the energy transfer of 60 meV. With MAPS it is possible to determine the dynamical structure factor $S(\mathbf{Q},\omega)$, where $\mathbf{Q}$ is the momentum transfer and $\hbar\omega$ is the energy transfer, in three dimensions (energy and two momentum transfer axes). Using the Mslice program by Coldea (ISIS) the data were first projected on various two-dimensional slices to inspect the overall picture, and then the phonon dispersions and scattering intensities were determined from the constant-$\mathbf{Q}$ energy cuts by peak fitting after removing the background including the multiphonon contribution.

The $YBa_2Cu_3O_{6.95}$ sample prepared at the University of Washington (sample 1) was a disk-shaped crystal weighing 105 grams with $T_C = 93$ K. The incident energy of 117.5 meV was used for the measurement of this sample. The sample was placed in a closed-cycle refrigerator (displex) with one of the twinned a/b axis and the *c* axis on the horizontal plane, and the other a/b axis in the vertical position. The *c* axis was rotated 41° away from the incident-beam direction towards the high-angle detector bank on the hori-

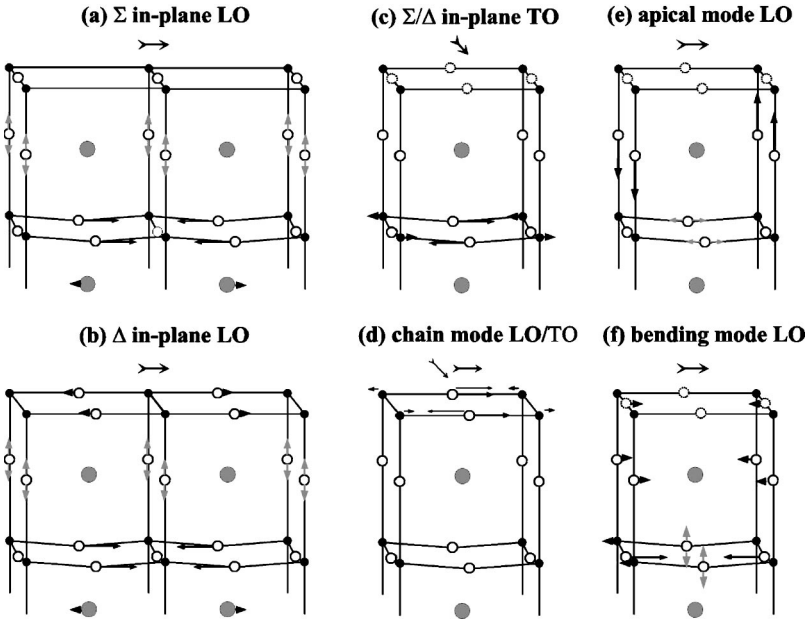

FIG. 1. Schematics of atomic displacement for each phonon mode at the zone boundary, with a black circle denoting Cu, a white circle O, and a gray circle Y and Ba. The Cu-O chain is at the top of each figure, and one of the two CuO_2 planes is shown below. A dark arrow attached to an atom indicates a primary polarization direction, a gray arrow indicates a secondary polarization which is phase shifted by π, and a thin arrow in (d) indicates a polarization of a transerve mode.

zontal plane. In the following we use the (h, k, l) notation to express $\mathbf{Q}$ with the units of the reciprocal lattice vectors in the a/b in plane, a/b vertical, and c directions, respectively. The vertical angle range ($\pm 5°$) of the high-angle detector bank limited the coverage in the k direction to only the central half of the Brillouin zone, i.e., k up to ± 0.25. Another set of data were taken with the c axis parallel to the incident neutron beam. This setting results in a considerable c axis component of $\mathbf{Q}$, and was used to assess the apical-oxygen modes. Detailed analysis of this set of data will be reported elsewhere. A separate measurement was made with a $YBa_2Cu_3O_{6.95}$ sample grown at ISTEC (sample 2), which consisted of 30 aligned single crystals weighing in total of 31.7 g.[15] In this measurement the sample was rotated around the c axis by 4.8° to cover the entire half of the Brillouin zone, $k=0-0.5$. Also, a slightly different incident energy of 124.7 meV was chosen to cover the $\mathbf{Q}-\omega$ space that fell on the gaps of the detector banks in the first measurement. Both samples were fully twinned. Detwinned single crystals of sufficient quantity for phonon measurements with MAPS are not presently available. While sample 1, grown with the flux method, had about 10% of a nonstoichiometric impurity phase (the so-called green phase), sample 2, grown from the melt, had almost none of this phase. As far as the phonon dispersions are concerned there was no discernible major difference between the two samples. Additional measurements were performed on sample 1 by triple-axis spectroscopy with the HB-2 and HB-3 instruments at the high-flux isotope reactor (HFIR) at the Oak Ridge National Laboratory. For the triple-axis measurements the final energy was fixed at 14.87 meV and the sample-to-detector horizontal collimation elements were 48′-60′-40′-120′.

We focused our attention on the Cu-O bond-stretching-type phonons propagating along the a/b axes in the twinned crystal. The high-energy bond-stretching phonons of interest are oxygen modes mainly polarized in the CuO_2 plane, as shown schematically in Fig. 1. Since modulation of the Cu-O distance results in charge transfer between Cu and O, this mode is expected to show strong electron-phonon coupling.[16–18] $YBa_2Cu_3O_{6.95}$ has an orthorhombic structure with the CuO chains running along the b direction. In the reciprocal space a direction is labeled Σ and b direction Δ according to standard notation.[19] Previous measurements have shown that the LO modes have strongly reduced frequencies compared to the insulating parent compound $YBa_2Cu_3O_6$ in the outer half of the Brillouin zone along a/b direction.[3,4] Due to the presence of the Cu-O chains, some degree of anisotropy is expected in the lattice dynamics in the CuO_2 plane from orthorhombicity. At the Brillouin-zone center, Raman scattering on detwinned single crystals has identified that the B_{2g} (a axis polarization) and B_{3g} (b axis) bond-stretching modes are split by 7 meV.[20] We note that the displacements of the chain oxygen modes parallel to the planes are not Raman active, except perhaps weakly due to disorder, therefore the above mode assignments must be correct. This splitting is also confirmed by neutron scattering on twinned crystals[21] and the results presented here.

Figure 2 shows the h-ω cut around the reciprocal lattice point $\mathbf{Q}=(h,k,l)=(3,0,l)$ (in the units for the Q_x and Q_y axes of the provisional tetragonal reciprocal lattice constant of $2\pi/\bar{a}=1.629$ Å^{-1}, where $\bar{a}$ is the average between $a=3.831$ Å and $b=3.895$ Å of the orthorhombic lattice) for sample 1 at $T=110$ K. The data were integrated along k from -0.1 to 0.1. The l index changes with energy, because only a three-dimensional surface of the four-dimensional space is determined by one measurement. In the present setting the c axis was rotated by 41° so that the energy transfer $\hbar\omega=74$ meV corresponds to $\mathbf{Q}=(3,0,1.8)$ for sample 2. Since $c/d\sim 3.6$, where d is the spacing between the double CuO_2 layers, only the u modes that are symmetric for the two layers are seen with $l\sim 0$ (~ 50 meV), while only the g modes that are antisymmetric are seen at $l\sim 1.8$ (~ 70 meV). In this paper the l dependence is neglected and we use the two-dimensional notation (h, k) below for sim-

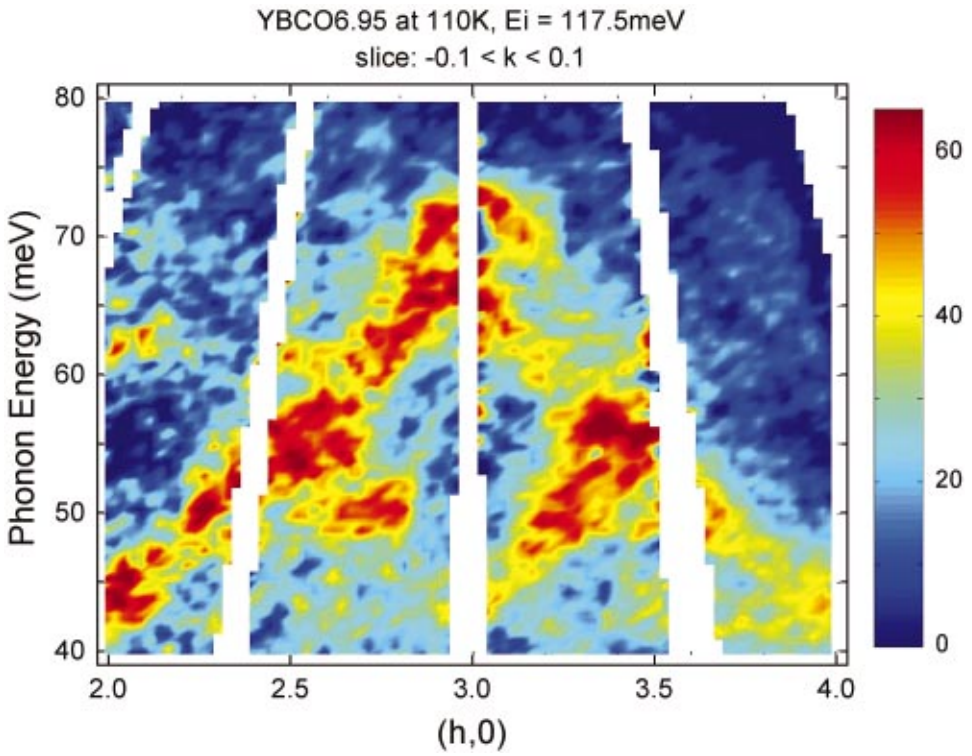

FIG. 2. (Color) $S(\mathbf{Q},\omega)$ of $YBa_2Cu_3O_{6.95}$ at $T=110$ K determined by the MAPS. The horizontal axis is the h index, with $\bar{a}^* = 2\pi/\bar{a} = 1.629$ Å^{-1}. Data were integrated from $k=-0.1$ to 0.1, and l changes with energy as discussed in the text. White gaps are due to gaps in the detector coverage. Data were binned to a mesh grid with $\Delta h = 0.025$ and $\Delta E = 0.5$ meV, and then smoothed once by weighted 3×3 adjacent averaging.

plicity, since earlier data[3–6] and our measurements made at HFIR suggested that the l dependence is weak due to the layered nature of the compound.[22] The data presented in Fig. 2 are corrected for the background including multiphonon scattering, Q^2/ω, thermal population, the Debye-Waller factor, and k'/k phase-space factor, where k and k' are the initial and final neutron wave numbers.

In the slice presented in Fig. 2 mainly the LO phonons along the twinned a/b axis are observed, since the neutron-scattering intensity is proportional to $(\mathbf{Q}\cdot\boldsymbol{\epsilon})^2$, where $\boldsymbol{\epsilon}$ is the phonon polarization. In Fig. 2 two phonon branches are seen near (3, 0) and 70 meV. One has the dispersion maximum at 72 meV around (3.03, 0), while the other at 66 meV at (2.97, 0). The slight misalignment of the maxima of the dispersion with the nominal zone center (3, 0) must be due to the fact that a is smaller than b by 2%. Thus we find that the 72-meV mode propagates along Σ (a direction) while the 66-meV mode propagates along Δ. This assignment agrees with the Raman result at the zone center which identified these modes to be the B_{2g} and B_{3g} modes, respectively.[20] Thus we will use $2\pi/a$ and $2\pi/b$ as the units of the indices below, unless noted otherwise. The phonon splitting due to orthorhombicity is consistent with the higher-frequency mode having a shorter unit-cell distance.

The large frequency offset of the Δ and Σ branches allows us to follow each mode independently, in spite of the fact that the crystal is twinned. A typical energy cut, the intensity at a fixed (h, k) as a function of energy, is given in Fig. 3. The dispersion and the scattering intensity of these modes were determined by fitting Gaussian peaks to the energy-cut data in the range $2.5<h<3.5$. Since a large number of peaks, up to 7, are involved, we used the data from other parts of the Q space as well as another data set as a guide. First the dispersion of the Cu-O bond-bending mode was determined from the cuts taken in the range $h<2.5$ or $3.5<h$, where the bond-stretching mode intensity is reduced and barely seen. Similarly the apical-oxygen modes were determined from the second set of data obtained with the c axis parallel to the incident beam ($\Theta=0$).

In the fitting procedure the peak width was fixed to the values calculated for resolution, and also the number of peaks was fixed (seven in the range seen). In the range $2.5<h<3.5$ small peaks due to the apical-oxygen modes were compared to the dispersion previously determined from the

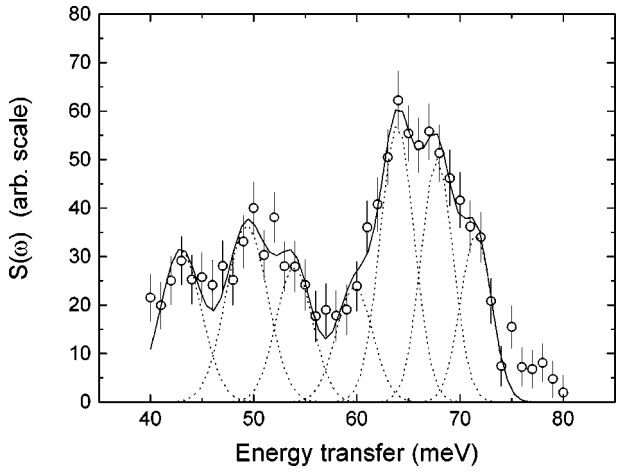

FIG. 3. A constant-$\mathbf{Q}$ cut at $\mathbf{Q}=(2.85,0)$ as a function of energy. Data were integrated for k from -0.1 to 0.1, h from 2.8 to 2.9. The intensity was fit with multiple Gaussian peaks with the width varying with energy reflecting the energy-dependent resolution. The subpeak at 61 meV is due to the c-axis apical-oxygen mode.

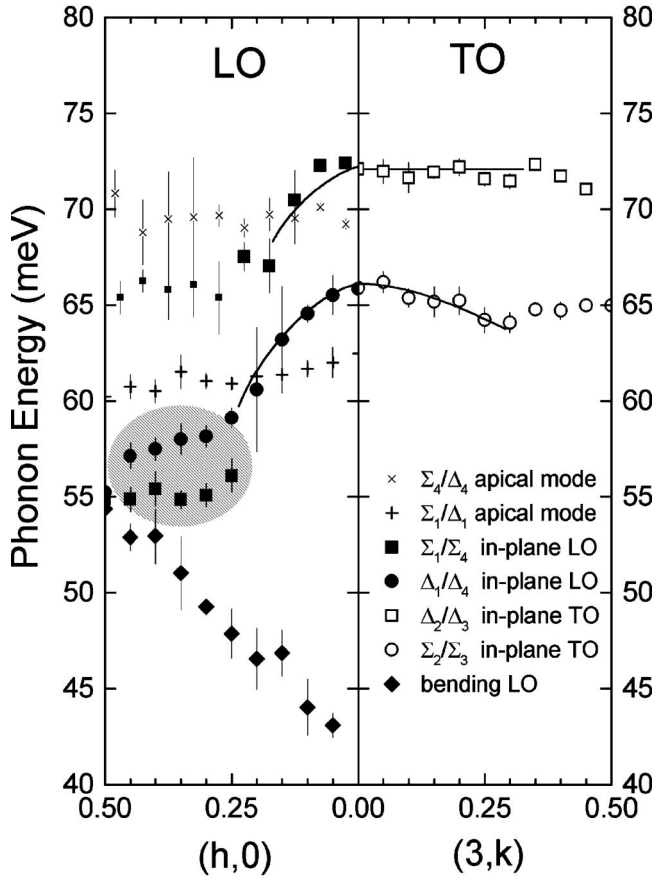

FIG. 4. Phonon dispersion of the Cu-O bond stretching and Cu-O bond-bending modes in $YBa_2Cu_3O_{6.95}$. The left side shows the LO phonons and the right side the TO phonons. Small symbols indicate low intensity. The mode around 70 meV is tentatively assigned to the apical-oxygen mode. Note that the units of $2\pi/a$ were used for the Σ modes, and $2\pi/b$ for the Δ modes.

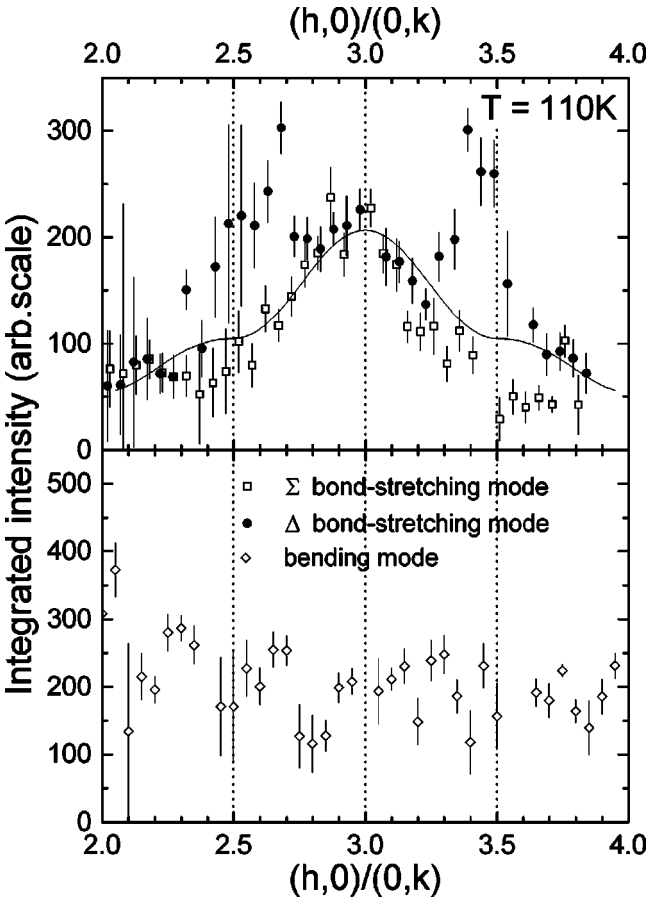

FIG. 5. Intensity of the Cu-O bond-stretching LO phonons for $YBa_2Cu_3O_{6.95}$ obtained by peak fitting, at $T=110$ K. The solid line indicates the structure factor for a shell model for the Σ mode. Since it is difficult to separate the low-energy Σ LO branch at 55 meV from the Δ LO branch near the zone boundary, the total intensity for the low-energy Σ LO branch and the Δ LO branch is shown.

data with $\Theta=0$, and their positions were corrected when necessary. The continuity of the peak fitting results as a function of q indicates a success of fitting, in spite of a relatively large number of peaks to fit.

As shown in the left panel of Fig. 4 the Σ LO branch disperses from 72 meV to 67 meV near the (0.25, 0) point, but beyond this point the intensity rapidly decreases. The Δ LO branch disperses from 66 meV down to 57 meV near the zone boundary, where it mixes with an intense flat mode around 55 meV. Mode assignment is difficult in the area near the zone boundary at 55–57 meV, but since the 57 meV mode is more symmetric around (2.97, 0) than (3.03, 0) we tentatively identify this mode as the Δ branch. The 55-meV branch is identified as the second Σ LO branch as we discuss below. In addition two weak branches are present in the energy ranges of about 70 meV and 61 meV, which we identify as the IR-active and Raman-active apical-oxygen modes, respectively, polarized along c. The basis of this identification is the second set of data taken with the c axis parallel to the incident beam, in which the c axis modes are more clearly seen. These data will be discussed elsewhere. Finally the oxygen bond-bending mode is observed in the energy range of 40–55 meV. These branches were clearly separated from the CuO_2 plane Δ and Σ branches except in the close vicinity of the zone boundary ($0.47<h<0.53$). The intensity of this mode at the zone boundary was estimated by extrapolation, and was separated from that of the bond-stretching mode.

The intensities of the Δ and Σ LO branches at $T=110$ K, determined from the area under the fitted peak, are given in Fig. 5 from $h=2.0$ to 4.0. For the Σ LO branch only the intensity of the high-energy mode (65–72 meV) is plotted. Since it is difficult to separate the intensities of the Δ and Σ modes at 55–57 meV, in Fig. 5 the sum of the intensities for the two modes is shown. The figure also shows the intensity of the Cu-O bond-bending mode, which depends on q only weakly. Thus the separation of the intensity of this mode from those of the bond-stretching modes is not difficult. The Cu-O bond-stretching modes are composed mostly of oxygen displacements with a small contribution from Cu displacements which are opposite in direction to oxygen displacements. The intensity (structure factor) varies with $\mathbf{Q}$, since at $\mathbf{Q}=(3,0)$ the oxygen and copper displacements add themselves to the structure factor, while at $\mathbf{Q}=(4,0)$ and (2,

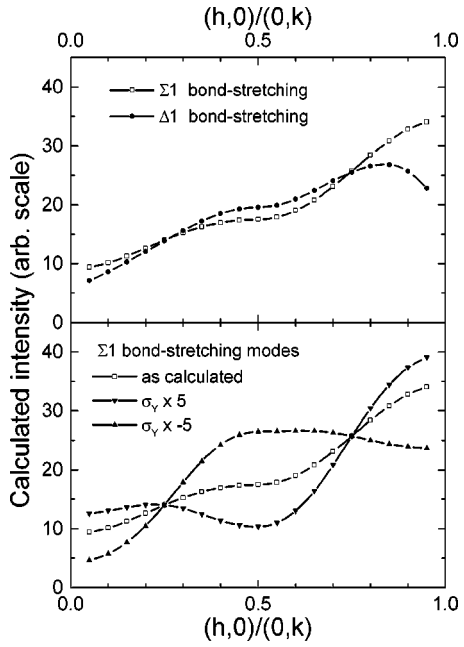

FIG. 6. (a) Intensity of the Cu-O bond-stretching LO phonons calculated for a shell model along *a* and *b* directions,[23] (b) calculated intensity with the amplitude of yttrium displacement artificially increased by a factor of 5, with the displacement parallel or antiparallel to oxygen.

0) they subtract from each other. While the Cu displacement is small, the neutron-scattering length of Cu is nearly twice as much as that of oxygen, resulting in significant decrease in intensity going from (3, 0) to (4, 0) or (2, 0).

The shell model by Kress *et al.*[23] predicts vanishing intensities at (2, 0) and (4, 0), which disagrees with the observation. The model was then modified by reducing the amplitude of copper by 50% to fit the amplitudes at these points. This modification does not change the intensity substantially otherwise, and predicts a smoothly varying intensity shown also in Fig. 5. The model gives almost equal intensities for the Σ mode and the Δ mode as shown in Fig. 6(a), while the intensity determined from the data is highly anisotropic. It is too low or too high compared to the model intensity for the Σ mode and the Δ mode, respectively, in the vicinity of the zone boundary. The loss of the intensity of the Σ mode may be explained by a model, for instance, if the amplitude of displacement for yttrium is artificially increased by a factor of 5, as shown in Fig. 6(b). However, to explain the increase in intensity for the Δ mode yttrium has to move in the opposite direction with respect to oxygen for the Δ mode [Fig. 6(b)]. Since yttrium is farthest from the chain it is difficult to believe that the motion of yttrium has to be opposite along *a* and *b* directions. Also at such a high frequencies the amplitude of yttrium compared to that of oxygen cannot be so large. In addition the calculated curves in Fig. 6(b) have nodes at $h=0.25$ and 0.75, while the data do not show such nodes. Thus it appears to be difficult to explain the observed intensity based only upon the phonon structure factor.

An alternative explanation is that the second, low-energy branch of the Σ mode exists at 55-meV near the zone boundary as indicated in Fig. 4, and a significant portion of the spectral intensity of the high-energy mode is transferred to this low-energy mode. Similar mode splitting of the bond-stretching LO mode has been observed for $La_{1.85}Sr_{0.15}CuO_4$ (Ref. 5) and also for $La_{1.69}Sr_{0.31}NiO_4$.[24]

The in-plane anisotropy was noted also in a recent paper by Pintschovius *et al.* for $YBa_2Cu_3O_{6.6}$ [O(6.6)] composition.[25] They, however, did not consider the possibility of branch splitting of the Σ mode. Our previous study on the composition dependence of the dispersion shows that the intensity of the low-energy branch increases with hole doping,[12] so that for O(6.6) the intensity transfer must be only about a half of what is observed for O(6.95) here. For this reason it is not surprising that the authors of Ref. 25 did not consider this possibility, since it is more difficult to see the intensity transfer for O(6.6).

Thus the dispersion of the LO modes is very anisotropic even within the CuO_2 plane, with the Σ mode splitting into two branches. Anisotropy is less apparent in the transverse (TO) modes emanating from the B_{2g} and B_{3g} phonons. The dispersions of the transverse modes were determined by the k-ω cut near the (3, 0) point. In the k-ω cut the phonon

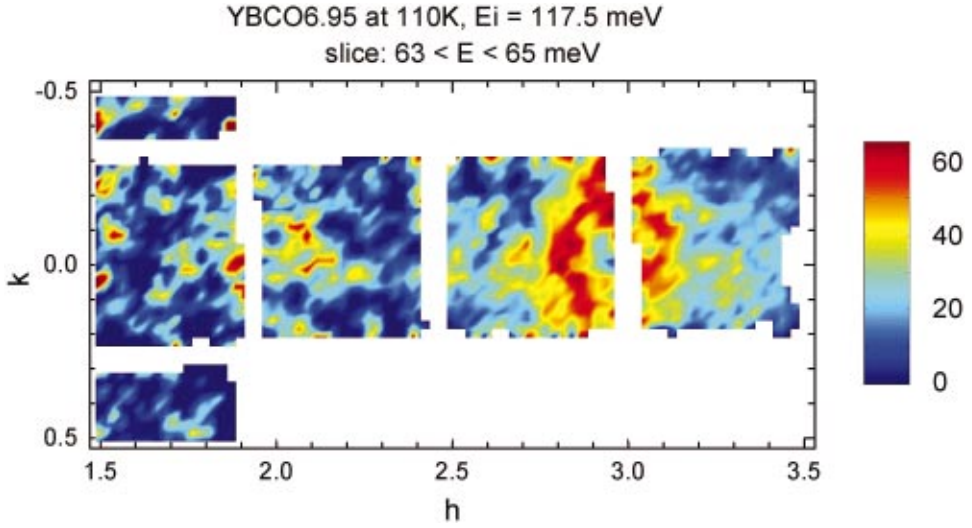

FIG. 7. (Color) The constant energy cut at $\hbar\omega=64$ meV (integrated from 63 to 65 meV) showing a ring around the zone center, suggesting that the TO of the Σ branch and the LO of the Δ branch have a similar dispersion.

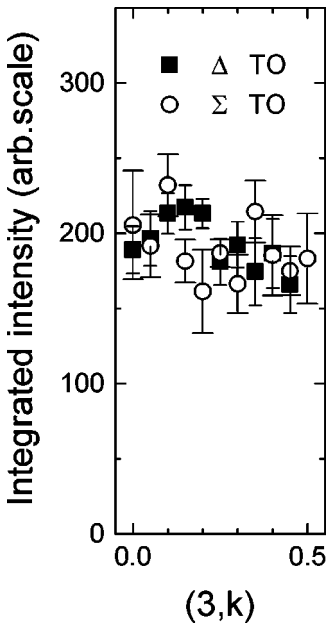

FIG. 8. The intensity of the in-plane Δ and Σ TO modes.

momentum, $\mathbf{q}=\mathbf{Q}-\mathbf{K}$, where $\mathbf{K}$ is the reciprocal lattice vector, is nearly perpendicular to $\mathbf{Q}$. Thus mainly transverse phonons are seen in the k-ω cut. Because the result for sample 1 covered only up to about $k\sim\pm0.25$, the data for the outer half of the Brillouin zone were obtained only for sample 2 which was rotated around the c axis by 4.8° to cover a half of the Brillouin zone, $k=0$–0.5. The dispersion of the transverse modes thus determined is shown in the right-hand side of Fig. 4. The transverse mode along Δ (with polarization along the a direction) remains dispersionless at 72 meV, while the transverse mode along Σ disperses more, from 66 meV at the zone center to 64 meV at $k=0.25$, and up to this point the dispersion of the TO mode is similar to that of the LO mode. Indeed the constant-energy slice at 64 meV (Fig. 7) shows a ring of high intensity, suggesting that the dispersion is similar for the both. Beyond $k=0.25$ the Σ TO mode is also nearly dispersionless. The k dependence of the intensity is very similar for the Δ and Σ modes as shown in Fig. 8. It is important to note that the Σ TO branch, unlike the Σ LO branch, does not split into two.

The dispersions of the bond-stretching phonon branches appeared to show no clearly identifiable temperature dependence. But the scattering intensity was found to show significant changes with temperature, beyond what is expected for thermal excitation. This is shown in Fig. 9 as the difference in $S(\mathbf{Q},\omega)$, in the units of $2\pi/a$, between 7 K and 110 K for sample 1 after the correction for the Bose-Einstein factor. Note that some strong intensities near the edges of the detector banks are artifacts due to the edge shadowing. A very similar result was obtained for sample 2, and with the triple-axis spectrometer at HFIR for sample 1 (Fig. 10).[26] There is a transfer of the neutron-scattering intensity from the mid-energy range 60–68 meV to the high-energy range (70–73 meV) and the low-energy range (50–60 meV). In particular the increase in the intensity of the TO mode in the low-energy range is nearly dispersionless around 60 meV, but that of the LO mode takes place in the band that spans from around 60 meV at the zone center to 50 meV at the zone edge. This band parallels the dispersion of the b-axis LO mode, Δ mode. The mirror symmetry plane of this band for the LO mode is slightly below $h=3.0$ in the units of $2\pi/\bar{a}$, which identifies this band with the Δ mode. Indeed the loss of intensity occurs most conspicuously from the ω–$\mathbf{Q}$ range for the b-axis polarized Δ LO and Σ TO modes. Furthermore

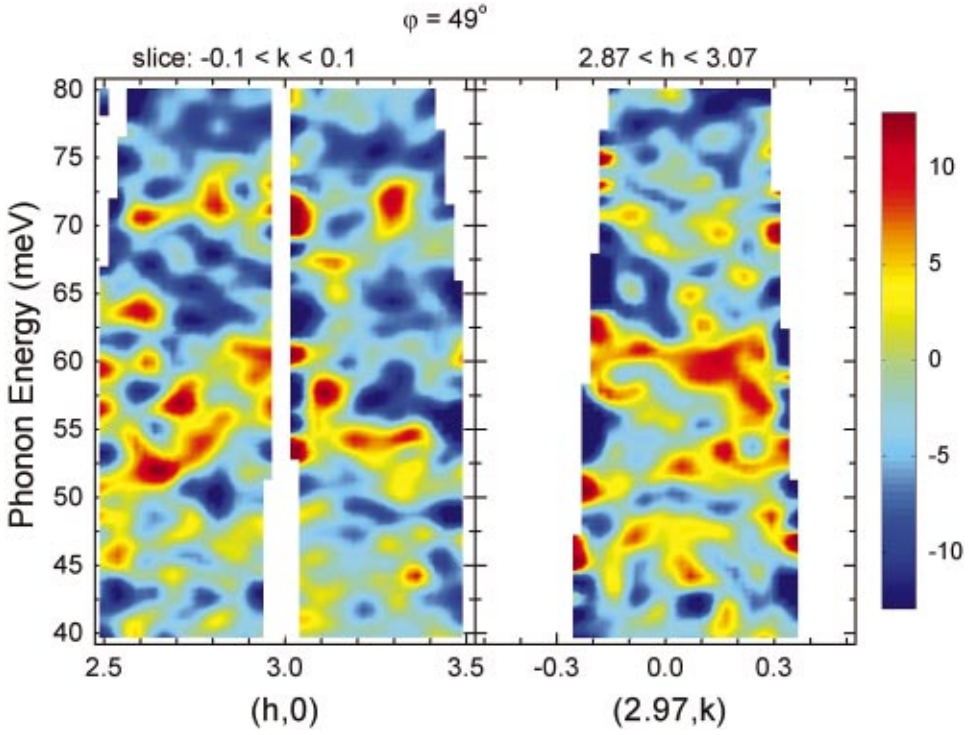

FIG. 9. (Color) Difference in $S(\mathbf{Q},\omega)$ for $YBa_2Cu_3O_{6.95}$ between $T=7$ K and 110 K, $S(T=110\text{ K})-S(T=7\text{ K})$, for the ω-h slice at $k=0$, (integrated from $k=-0.1$ to 0.1, left) and the ω-k slice at $h=2.97$ (integrated from $h=2.87$ to 3.07, right). The units of $2\pi/\bar{a}$ were used for h and k in this plot and the data were smoothed four times. As temperature is reduced the intensity is transferred from the energy range 60–70 meV to the energy ranges above and below.

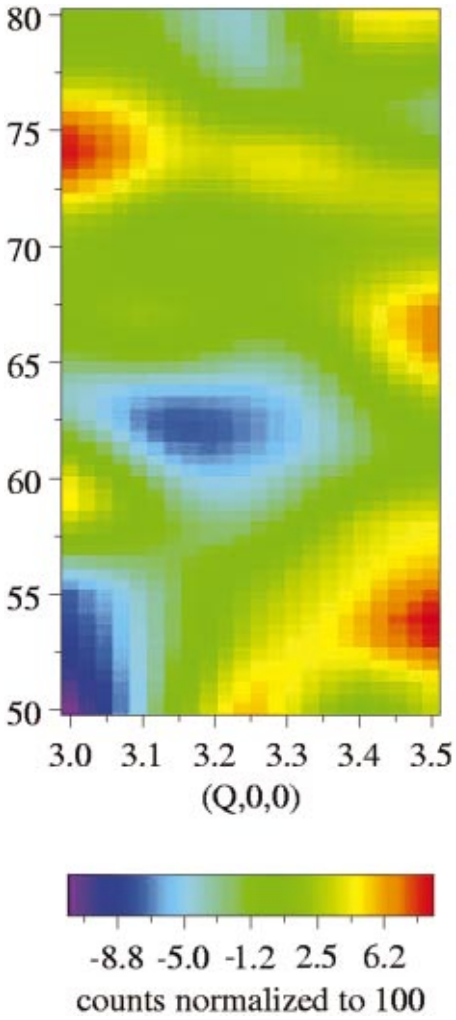

FIG. 10. (Color) A similar result obtained for the ω-h slice with the triple-axis spectrometer at the HFIR.

the ω-k slice for the TO mode shows a larger change when it is integrated from $h=2.87$ to 3.07 (Σ TO) rather than from $h=2.93$ to 3.13 (Δ TO). For these reasons we tentatively conclude a part of the spectral weight of the b-axis polarized Δ LO and Σ TO branches is transferred to this new branch as the temperature is lowered. The new Δ LO and Σ TO branch is uniformly softened by about 6 meV compared to the original branch. However, this conclusion needs to be confirmed by a measurement with an untwinned sample.

The fraction of the transferred intensity is about 20–25 %, judged from the intensity change. In order to determine the temperature dependence of this transfer in the spectral weight we measured $S(\mathbf{Q},\omega)$ at $\mathbf{Q}=(3.25,0,0)$ for sample 1 with the triple-axis spectrometer at HFIR as a function of temperature, as shown in Fig. 11. It is clear that as temperature is lowered below 100 K the intensity in the range 60–65 meV is decreased, while that in the range 51–55 meV is increased. The difference in the average intensity between the range 1 (56–68 meV) and the range 2 (51–55 meV), $I(2)-I(1)$, is shown in Fig. 12. It has an obvious resemblance to the temperature dependence of the superconducting order parameter, suggesting an intimate

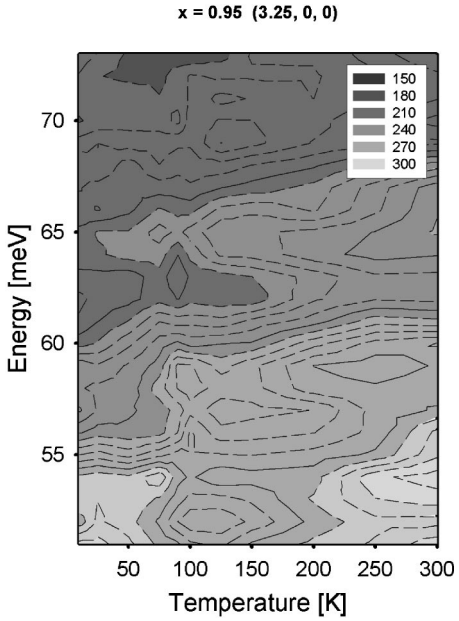

FIG. 11. Inelastic scattering intensity at $\mathbf{Q}=(3.25,0,0)$ as a function of temperature, determined with the triple-axis spectrometer at the HFIR. Data were smoothed once to reduce noise.

connection between the superconductivity in this compound and the Cu-O bond-stretching phonons.

III. ANALYSIS AND DISCUSSION

The results discussed above confirm the strong softening of the in-plane Cu-O bond-stretching LO mode observed previously for YBCO (Refs. 3,4) and LSCO.[3–6] In order to explain this softening in terms of the regular von-Kármán-type lattice dynamics one has to introduce strong oxygen-oxygen attraction within the CuO_6 octahedron,[5] which is rather counterintuitive since oxygen ions are negatively charged. In contrast the TO modes do not show such strong softening. The a-polarized mode is dispersionless, while the b-polarized TO mode shows slight dispersion. A possible explanation of this marked difference between the LO and TO modes is that the LO mode softening is an electronic effect, for instance, through the dielectric constant $\epsilon_{el}(\mathbf{q},\omega)$. As in

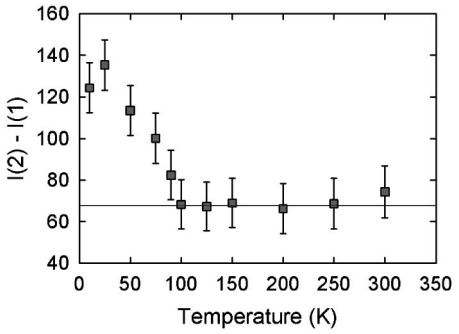

FIG. 12. Temperature dependence of the intensity difference I_2-I_1, where I_1 is the average intensity in Fig. 10 from 56 to 68 meV, I_2 from 51 to 55 eV, at $\mathbf{Q}=(3.25,0,0)$. Data were taken with the triple-axis spectrometer at the HFIR.

the case of the well-known Lyddane-Sachs-Teller relationship for an insulator, only the LO mode is renormalized by the internal electric field. Indeed such a dielectric effect was proposed by Tachiki and Takahashi.[27] They suggested that the LO phonon softening can be explained in terms of a negative electronic dielectric function due to overscreening involving the vibronic state, in which charge and lattice vibrate at the same frequency with an opposite phase. According to their theory the frequencies of the LO and TO modes are related by

$$\omega_{LO}^2(q)=\omega_{TO}^2(q)+\frac{A}{\epsilon_{el}(q,\omega_{LO}(q))}, \tag{1}$$

where $A=\omega_{LO}^2-\omega_{TO}^2$ for the insulator. While $\epsilon_{el}(\mathbf{q}=0,\omega_{LO})=\infty$ reflecting its metallicity, $\epsilon_{el}(\mathbf{q},\omega)$ becomes negative above the Fermi momentum k_F due to overscreening. This theory predicts high-temperature superconductivity due to strong resonant electron-phonon coupling.[27] The phonon softening was explained also in terms of the changes in the electron energy in the Hubbard model.[16,17] More recently a microscopic explanation of the overscreening effect was proposed using the Hubbard model, through the negative Born effective charge due to the phonon-induced charge transfer.[28] The electronic nonlocal interaction was considered also by Falter *et al.* using a screening model based upon the local density approximation calculation.[18] The relationship among these models will be discussed in detail elsewhere.

Our experimental results suggest strong in-plane anisotropy of the bond-stretching mode. The softening of the mode at the zone edge compared to the zone center is larger for the *a*-axis mode LO branch (17 meV) than for the *b*-axis mode LO branch (9 meV). However, the *a*-axis mode is also split into two branches, a high-energy (65–72 meV) branch and a low-energy (55 meV) branch. Furthermore, Fig. 5 seems to suggest that not all the intensity near the zone boundary is transferred from the high-energy Σ branch to the low-energy $\Sigma+\Delta$ branch, since the intensity of the high-energy Σ branch is not zero at the zone boundary. This implies that there must be two types of local environment, with nearly equal population, for instance, with and without local charge.

The anisotropy in the dispersion, in particular, the branch splitting along the *a* axis, does not appear to be explained by the orthorhombic distortion and the presence of the Cu-O chain along the *b*-direction. As we mentioned earlier a very similar branch splitting was observed for doped nickelate, $La_{1.69}Sr_{0.31}NiO_4$.[24] In this case the splitting occurred along the $[h, h, 0]$ direction. Since the direction of the branch splitting coincides with that of the charge stripes for each case, $[h, 0, 0]$, for the cuprates and $[h, h, 0]$ for the nickelates, this invites an interesting speculation that the branch splitting is caused by, or at least a signature of, the charge stripes. In nickelates the presence of charge stripes is well established. In superconducting cuprates, however, it is merely a speculation at this moment. In either case it appears to be most natural to relate the branch splitting to some spatial charge inhomogeneity, such as charge stripes.

The temperature dependence shown in Fig. 12 suggests that the softening of the Cu-O bond-stretching mode may be related to superconductivity. The difference in the dynamic structure factor between $T=110$ K and 7 K shown in Figs. 8 and 9 indicate that below T_c about $20-25\,\%$ of the spectral weight of the Δ branch is shifted to the new low-energy branch in the energy range of 50–60 meV. This suggests that the spatial inhomogeneity of charge distribution develops both in the *a* and *b* directions, which may be related to the two-dimensional nature of superconducting correlation.[29,30] The exact nature of the low-energy Δ branch is unknown at present, but it is interesting that its energy maximum ($\sim$60 meV) corresponds to the energy of the apical-oxygen mode, suggesting some role of apical-oxygen ions. The *c*-axis motion of apical-oxygen couples to charge through the Jahn-Teller effect, as originally envisaged by Bednorz and Müller.[31]

The possible presence of inhomogeneous electron dynamics, such as the spin/charge stripes, has an important implication to the electron-phonon coupling.[32] While the Cu-Cu electron transfer energy is of the order of 0.5 eV, far higher than the phonon energy, the electron tunneling across the spin stripes must be much reduced. This could bring the energy scale of electrons down, particularly around the extended saddle point,[33] possibly to the level comparable in energy to the LO phonons. This makes the possibility of the vibronic overscreened resonant coupling, as proposed by Tachiki and Takahashi,[27] much more realistic.[34] Other related or overlapping electron-phonon models, such as the resonant two-band mechanism by Bussmann-Holder,[35] the phonon umklapp mechanism by Castro Neto,[36] and the coupled spin-ladder mechanism of Sachdev,[37,38] may offer alternative description of some parts of the observed phenomenon. The interaction between the in-plane LO mode and the apical-oxygen mode mentioned above suggests possible relevance of the two-band model.[35]

For $La_{1.85}Sr_{0.15}CuO_4$ (LSCO) both the split dispersion[5] as well as a continuous dispersion[39] have been observed, suggesting that both of them exist in LSCO just as in YBCO. Then the anisotropy in the screening may be a common feature of the cuprate superconductors, not a byproduct of the chain. In YBCO, the orthorhombicity and the presence of the chain must favor the alignment of stripes in one direction (*b* axis) throughout a twin domain, while in LSCO two types of domains with stripes along *x* and *y* must coexist.

ACKNOWLEDGMENTS

The authors would like to thank L. Pintschovius, J. Tranquada, M. Tachiki, A. Lanzara, N. Nagaosa, A. R. Bishop, A. Bussmann-Holder, A. H. Castro Neto, S. Sachdev, S. Kivelson, D. Mihailovic, J. C. Phillips, and P. Allen for helpful discussions, and Y. Fudamoto, S. Koyama, and Y. Shiohara for their help in preparing crystals. This work was supported by the National Science Foundation under Grants No. DMR96-28134 and DMR01-02565 to the University of Pennsylvania and the U.S. Department of Energy under Contract No. W-7405-Eng-36 with the University of California.

The crystal growth at ISTEC was supported by the New Energy and Industrial Technology Development Organization as Collaborative Research and Development of Fundamental Technologies for Superconductivity Applications.

[1] See, for example, P.W. Anderson, *The Theory of Superconductivity in the High-T_C Cuprates* (Princeton University Press, Princeton, 1997).
[2] T. Egami and S.J.L. Billinge, in *Physical Properties of High Temperature Superconductors V*, edited by D. Ginsberg (World Scientific, Singapore, 1996), p. 265.
[3] L. Pintschovius, N. Pyka, W. Reichardt, A.Yu. Rumiantsev, N.L. Mitrofanov, A.S. Ivanov, G. Collin, and P. Bourges, Physica C **185-189**, 156 (1991).
[4] L. Pintschovius and W. Reichardt, in *Physical Properties of High Temperature Superconductors IV*, edited by D. Ginsberg (World Scientific, Singapore, 1994), p. 295.
[5] R.J. McQueeney, Y. Petrov, T. Egami, M. Yethiraj, G. Shirane, and Y. Endoh, Phys. Rev. Lett. **82**, 628 (1999).
[6] R.J. McQueeney, J.L. Sarrao, P.G. Pagliuso, P.W. Stephens, and R. Osborn, Phys. Rev. Lett. **87**, 077001 (2001).
[7] P.V. Bogdanov, A. Lanzara, S.A. Kellar, X.J. Zhou, E.D. Lu, W.J. Zheng, G. Gu, J.-I. Shimoyama, K. Kishio, H. Ikeda, R. Yoshizaki, Z. Hussain, and Z.X. Shen, Phys. Rev. Lett. **85**, 2581 (2000).
[8] A. Lanzara, P.V. Bogdanov, X.J. Zhou, S.A. Keller, D.L. Feng, E.D. Lu, T. Yoshida, H. Eisaki, A. Fujimori, K. Kishio, J.-I. Shimoyama, T. Noda, S. Uchida, Z. Hussain, and Z.-X. Shen, Nature (London) **412**, 510 (2001).
[9] J. Zaanen and O. Gunnarsson, Phys. Rev. B **40**, 7391 (1989).
[10] J.M. Tranquada, B.J. Sternlieb, J.D. Axe, Y. Nakamura, and S. Uchida, Nature (London) **375**, 561 (1995).
[11] H.A. Mook, P. Dai, F. Dogan, and R.D. Hunt, Nature (London) **404**, 729 (2000).
[12] T. Egami, in *Physics in Local Lattice Distortions: Fundamentals and Novel Concepts*, edited by Hiroyuki Oyanaki and Antonio Bianconi, AIP Conf. Proc. No. 554 (AIP, Mellville, NY, 2001), p. 38.
[13] T. Egami, R. J. McQueeney, J.-H. Chung, M. Yethiraj, M. Arai, Y. Inamura, Y. Endoh, S. Tajima, C. Frost, and F. Dogan, Appl. Phys. B (to be published).
[14] T. Egami, J.-H. Chung, R.J. McQueeney, M. Yethiraj, H.A. Mook, C. Frost, Y. Petrov, F. Dogan, Y. Inamura, M. Arai, S. Tajima, and Y. Endoh, Physica B **62**, 316 (2002).
[15] Y. Yamada and Y. Shiohara, Physica C **217**, 183 (1993).
[16] S. Ishihara, T. Egami, and M. Tachiki, Phys. Rev. B **55**, 3163 (1997).
[17] Y. Petrov and T. Egami, Phys. Rev. B **58**, 9485 (1998).
[18] C. Falter and G.A. Hoffmann, Phys. Rev. B **64**, 054516 (2001).
[19] O.V. Kovalev, *Representations of the Crystallographic Space Groups*, edited by H.T. Stokes and D.M. Hatch (Gordon and Breach Science Publishers, Langhorne, PA, 1993); Refs. 3,4 used the pseudotetragonal notation and called them Δ and Δ'.
[20] K.F. McCarty, J.Z. Liu, R.N. Shelton, and H.B. Radousky, Phys. Rev. B **41**, 8792 (1990).
[21] W. Reichardt, J. Low Temp. Phys. **105**, 807 (1996).
[22] Since the l index depends upon energy, symmetry of the mode changes with $\mathbf{Q}$ and $\hbar\omega$. For instance, the B_{3g} phonon mode connects to the Δ_4 branch at the zone center, but near the zone-boundary Y point (0, 0.5), as the energy moves down to 57 meV, the observed mode changes into the Δ_1 branch (B_{3u} mode). In spite of such changes in the l index, the observed dispersion agrees well with that measured for the u mode ($l=0$) at the HFIR, suggesting that the l dependence is either weak or absent. Thus in the following we suppress the suffix to indicate the mode symmetry.
[23] W. Kress, U. Schröder, J. Prade, A.D. Kulkarni, and F.W. de Wette, Phys. Rev. B **38**, 2906 (1988).
[24] J.M. Tranquada, K. Nakajima, M. Braden, L. Pintschovius, and R.J. McQueeney, Phys. Rev. Lett. **88**, 075505 (2002).
[25] L. Pintschovius, W. Reichardt, M. Kläser, T. Wolf, and H.v. Lö hneysen, Phys. Rev. Lett. **89**, 037001 (2002).
[26] T. Egami, R.J. McQueeney, Y. Petrov, M. Yethiraj, G. Shirane, and Y. Endoh, in *High Temperature Physics II*, edited by Stewart E. Barnes, Joseph Ashkenazi, Joshua L. Cohn, and Fulin Zuo, AIP Conf. Proc. No. 483 (AIP, Woodbury, NY, 1999), p. 38.
[27] M. Tachiki and S. Takahashi, Phys. Rev. B **38**, 218 (1988); **39**, 293 (1989).
[28] P. Piekarz and T. Egami (unpublished).
[29] E.W. Carlson and D. Orgad, Phys. Rev. B **62**, 3422 (2000).
[30] I. Martin, G. Ortiz, A.V. Balatsky, and A.R. Bishop, Europhys. Lett. **56**, 849 (2001).
[31] J.G. Bednorz and K.A. Müller, Z. Phys. B: Condens. Matter **64**, 189 (1986).
[32] J.C. Phillips, Int. J. Mod. Phys. B **15**, 3153 (2001).
[33] K. Gofron, J.C. Campuzano, A.A. Abrikosov, M. Lindroos, A. Bansil, H. Ding, D. Koelling, and B. Dabrowski, Phys. Rev. Lett. **73**, 3302 (1994).
[34] M. Tachiki, M. Machida, and T. Egami (unpublished).
[35] A. Bussmann-Holder, A. Müller, R. Micnas, H. Büttner, A. Simon, A.R. Bishop, and T. Egami, J. Phys.: Condens. Matter **13**, L169 (2001).
[36] A.H. Castro-Neto, J. Supercond. **13**, 913 (2000); cond-mat/0102281 (unpublished).
[37] S. Sachdev and N. Read, Int. J. Mod. Phys. B **5**, 219 (1991).
[38] K. Park and S. Sachdev, cond-mat/0104519 (unpublished).
[39] L. Pintschovius and M. Braden, Phys. Rev. B **60**, R15 039 (1999).